# Electrochemical and Spectroelectrochemical Behavior of the Main Photodegradation Product of Nifedipine: The Nitrosopyridine Derivative

**L. J. Núñez-Vergara,[1,2] S. Bollo,[1] J. Fuentealba,[1] J. C. Sturm,[1] and J. A. Squella[1]**

*Received November 19, 2001; accepted December 18, 2001*

***Purpose.*** To characterize the electrochemical behavior of the photodegradation product of nifedipine, i.e., 2,6-dimethyl-4-(2-nitrosophenyl)-3,5-pyridine-carboxylic acid dimethyl ester (NPD) in different electrolytic media. We also evaluated the interaction between free radicals generated from NPD and xeno/endobiotics.

***Methods.*** Tast polarography, differential pulse polarography, and cyclic voltammetry were used for the characterization. Controlled potential electrolysis and ultraviolet-visible spectroscopy were used to generate and to detect the nitroso radical anion.

***Results.*** In protic media, the NPD derivative gave a reversible well-defined peak either on Hg or glassy carbon electrodes in a reaction involving two electrons and two protons to give the hydroxylamine derivative. In mixed aqueous-organic media (pH 9) and in aprotic media, nitroso radical anion was isolated and characterized, exhibiting second-order dimerization rate constant ($k_2$) values of 11,300 ± 210 $[Ms]^{-1}$ and 8,820 ± 78 $[Ms]^{-1}$, respectively. Reactivity of the nitroso radical anion with relevant pharmacologic targets revealed a significant interaction with the tested endo/xenobiotics (cysteamine, GSH, *N*-acetylcysteine, and adenine).

***Conclusions.*** Both in mixed and aprotic media, NPD generated free-radical species, the nitroso radical anion. Taking into account their respective interaction rate constants, the following tentative rank order of reactivity can be established as follows: cysteamine > *N*-acetylcysteine > GSH > adenine.

**KEY WORDS:** nitroso pyridine derivative; nifedipine; cyclic voltammetry; nitroso radical anion; reactivity.

## INTRODUCTION

Nifedipine (dimethyl-1,4-dihydro-2,6-dimethyl-4-(2-nitrophenyl)-3,5-pyridine dicarboxylate) blocks $Ca^{2+}$ channels in myocardial and vascular smooth muscle cells, inducing vasodilatation and reduced peripheral resistance. These properties make nifedipine highly effective in the management of angina and arterial hypertension (1).

Nifedipine readily undergoes photolysis when exposed to short-wavelength (below 420 nm) visible or UVC (254 nm) radiation in aqueous solution, oxidizing to its 4-(2′-nitrosophenyl)-pyridine (NPD) or 4-(2′-nitrophenyl)-pyridine derivatives (2–4). Photolysis of nifedipine to the nitroso-pyridine derivative also results in a reversal of $Ca^{2+}$ channel blocking action in contracting ventricular muscle preparations *in vitro* (5). To protect against loss of therapeutic action, nifedipine tablets are stored in amber glass bottles and coated with visible ultraviolet (UV) radiation absorbing-reflecting film (6). Adverse skin reactions to the drug are rare, but there some reports suggesting that nifedipine may induce skin photosensitivity in some patients. Gibbs and co-workers (7) clearly demonstrated that nifedipine has a phototoxic potential that is mediated partially by the induction of a toxic nitroso-pyridine nifedipine photoproduct. Furthermore, Hayase (8) isolated several photodegradation products of nifedipine in tablets dispensed in the pulverized form by hospitals prescriptions containing the main photoproduct, dimethyl-2,6-dimethyl-4-(2-nitrosophenyl)-3,5-pyridine dicarboxylate (NPD).

In view of such antecedents, in this work we studied the electrochemic behavior of the main photoproduct from nifedipine, the nitrosopyridine derivative, and the feasibility of free-radical species formation in different electrolytic media. Their reactivities with some relevant biologic targets are also explored to support a possible mechanism of toxicity.

## MATERIALS AND METHODS

### Drugs and Reagents

Nitrosobenzene, dimethylformamide (DMF), pro-analysis grade, and tetrabutylammonium chloride (TBAC), were purchased from Merck Laboratories (Santiago, Chile).

### Preparation of NPD

Ninedipine solution (0.067 M) in acetone was irradiated with a UV lamp (UV-Black-Ray Lamp model B 100 AP, 366 nm filter) over 21 h with constant stirring and refrigeration by air circulation and a constant temperature of 20 ± 2°C. Photolysis products were separated by preparative thin-layer chromatography (Merck silica gel 60 $F_{254s}$ with a concentrating zone of 20 × 20 cm and thickness of 1 mm) using a developing solvent consisting of: petroleum ether/chloroform/acetone (50/30/20 v/v). The development was performed 3 to 4 times on a plate to separate photodegradation products. The separated band corresponding to NPD ($R_f$ = 0.59) was scraped and collected from plates. Then, it was extracted with two fractions of 25 mL of chloroform. Each chloroformic extract of the adsorbent was filtered and evaporated nearly to dryness and then was dissolved in 5 mL of methanol by heating and left to stand in a refrigerator overnight. Pale needles precipitated, which were collected and recrystallized several times from methanol.

The isolated product (pale greenish needles) exhibited the following characteristics: m.p. 93°C

IR (KBr): $\nu_{max}$ 30450, 3000, 2950, 2850, 1725, 1555, 1495, 1435, 1420, 1290, 1240, 1155, 1110, 1042, 960, 945, 850, 820, 780, 770, and 690 $cm^{-1}$

$^1$HNMR (300 MHz, $CDCl_3$): δ 2.66 (s, 6H, $CH_3$); 3.37 (s, 6H, $OCH_3$); and 6.48–7.68 (m, 4 H, aromatic-H)

GC-MS m/z (relative intensity): 328 (27, $M^+$), 311 (2, $M^+$ – OH), 298 (7, $M^+$ – NO), 284 (22), 269 (100, $M^+$ – $COOCH_3$,).

### *Differential Pulse Polarography (DPP)*

Experiments were performed in a Metrohm® 693 VA Processor equipped with a voltammetric stand 694 VA. A

[1] Laboratory of Bioelectrochemistry, Faculty of Chemical & Pharmaceutical Sciences, University of Chile, PO Box 233, Santiago, Chile.
[2] To whom correspondence should be addressed. (e-mail: lnunezv@ciq.uchile.cl)

0724-8741/02/0400-0522/0 © 2002 Plenum Publishing Corporation

Pentium III Gateway microcomputer was used for data control, acquisition, and treatment.

*Operating Conditions.* The operating conditions were as follows: pulse amplitude, 40 mV; potential scan, 4 $mVs^{-1}$; drop time, 1 s, voltage range, 0 to –2000 mV, current range, 1.25 to 5 μA, temperature, 25°C. All the solutions were purged with pure nitrogen for 10 min before the polarographic runs.

*Differential Pulse Voltammetry (DPV)*

Experiments were performed in a Metrohm® 693 VA Processor equipped with a voltammetric stand 694 VA. A Pentium III Gateway microcomputer was used for data control, acquisition, and treatment.

*Operating Conditions.* The operating conditions were as follows: pulse amplitude, 40 mV; potential scan, 4 $mVs^{-1}$; voltage range, 0 to –2000 mV, current range, 5 to 25 μA, temperature, 25°C. All the solutions were purged with pure nitrogen for 10 min before the voltammetric runs.

*Cyclic Voltammetry (CV)*

Experiments were performed in a Metrohm® assembly similar to that previously described in the above section. All cyclic voltammograms were performed at a constant temperature of 25°C. The solutions were purged with pure nitrogen for 10 min before the voltammetric runs. The return-to-forward peak current ratio, $I_{pa}/I_{pc}$, for the reversible first electron transfer (the NPD-NO/ NPD-NO·-couple) was measured, varying the scan rate from 0.1 $Vs^{-1}$ up to10 $Vs^{-1}$.

*Electrodes*

A Metrohm hanging mercury electrode (HMDE) with a drop surface of 1.90 $mm^2$ for C.V., a dropping mercury electrode (DME) for DPP and Tast P., and a glassy carbon electrode for DPV as working electrode and a platinum wire as a counter electrode were used. All potentials were measured against a Saturated Calomel reference electrode.

*Methods*

The experimental $I_{pa}/I_{pc}$ ratios were calculated according to Nicholson's procedure, using individual cyclic voltammograms (9). Kinetic reaction orders for the nitroso radical anion were quantitatively assayed for first- and second-order coupled reactions according to a previously published study (10–12). To quantitatively estimate the interaction rate constant ($k_i$) for the reaction between the nitroso radical anion generated from NPD and the endo/xenobiotics, we used a method previously developed in our laboratory (13). Endo/xenobiotics were dissolved in DMF and proper dilutions were done to obtain final concentration in the reaction media ranging between 0.01 mM and 5 mM.

*Controlled Potential Electrolysis (CPE).* CPE was performed on a platinum coil electrode or a glassy carbon electrode at –1000 mV in anhydrous acetonitrile containing 0.1 M tetrabutylammonium hexafluoro phosphate as supporting electrolyte. Oxygen was removed by pure, dry pre-saturated nitrogen. A three-electrode circuit with an Ag/AgCl electrode was used as reference. A Wenking potentiostat model POS 88 was used to electrolyze nitrosopyridine derivative (NPD).

*UV-Visible Spectroscopic Studies.* To obtain further information on the mechanism, mainly on the progress of the electrolysis, a UNICAM UV-3 spectrophotometer was used. UV visible spectra were recorded in the 220- to 800-nm ranges at different intervals. Acquisition and data treatment were performed with Vision 2.11 software. An electrolytic cell of our own construction (14), based on a 1-cm UV cuvette with a platinum coil as a working electrode was used for the *in situ* generation of the reduction species. The electrolyses were conducted under constant stirring, which was stopped before each measurement.

*Electrolytic Media*

*Aqueous Medium.* NPD was dissolved in 0.1 M Britton-Robinson buffer/ethanol: 70/30 + 0.3 M KCl to obtain the final concentration which varied between 0.1 mM and 1 mM.

*Mixed Medium.* From preliminary studies to obtain the optimal mixed media we have selected the following composition: 0.015 M aqueous citrate/DMF: 60/40, 0.3 M KCl and 0.1 M TBAC. NPD was previously dissolved in DMF.

*Aprotic Media.* NPD was dissolved in DMF containing 0.1 M TBAC. Final concentration varied between 0.1 mM and 1 mM.

**pH in Mixed Media**

pH measurements were corrected according to the following expression (15): $pH^* - B = \log U^0_H$, where pH* equals $-\log a_H$ in the mixed solvent, B is the pH meter reading and the term $\log U^0_H$ is the correction factor for the glass electrode. This factor was calculated at different mixtures of DMF and aqueous solvent, according to a previously reported procedure (16) and applied to our experimental pH determinations.

## RESULTS AND DISCUSSION

Taking into account that the photoproduct from nifedipine, NPD, probably is involved in toxicity reactions, we intended through an electrochemical approach to assess the feasibility of free radical formation and its potential reactivity with relevant pharmacologic targets. Therefore, the reduction behavior of NPD in different electrolytic media was mainly studied by cyclic voltammetric experiments to characterize the nitroso radical anion and its reactivity.

Stability studies on the NPD in the different electrolytic media were conducted. Results from these experiments demonstrated that the derivative was stable at least during 4 h with any variations either in current or potential values during this period.

**Protic Media**

NPD studies on Hg (DME) were not possible at pH < 7 because its reduction was masked by the mercury oxidation in 0.1 M Britton-Robinson buffer/0.3 M KCl/ethanol: 70/30. However, from pH 7 to 12, NPD exhibited a single well-defined signal by DPP and tast modes, which was shifted to more cathodic potentials with increasing pH. Also, by Tast polarography independence between the limiting current and pH was found indicating that the same number of electrons was transferred in this pH range. However, a systematic study

in the entire pH range was performed by using a glassy carbon electrode as the working electrode.

By DPV, NPD exhibited a single well-resolved peak in the pH range (Fig. 1A). Presumably, this peak corresponds to the well-described two-electron, two-proton reduction of nitroso derivative to the corresponding hydroxylamine derivative (17–20). Analyzing the evolution of the peak potential with the pH, three linear segments were found (Fig. 1A), with the following slopes: zone 1 (pH ≥ 2 to pH ≤ 5): 79.4 mV/pH, zone 2 (pH ≥ 6 to pH ≤ 8): 36.3 mV/pH and zone 3 (pH ≥ 8 to pH ≤ 12): 31.2 mV/pH. Probably, each linear segment represent a different mechanism according to a different sequences of addition of the electrons and protons to reach the overall two-electron, two-proton reduction of the nitroso to form the hydroxylamine [Eq. (1)] By using the reduction of nitrosobenzene as a pattern (17), we can assume the following different mechanism when passing from acidic to basic media: $H^+$ $e^-$ $H^+$ $e^-$ (zone 1), $e^-$ $H^+$ $H^+$ $e^-$ (zone 2), and $e^-$ $H^+$ $e^-$ $H^+$ (zone 3). Peak current was practically constant up to pH 6 (Fig. 1B), but at higher pH than pH 6 a significant increase was observed.

To complete the study of the electrodic mechanism of NPD in this media, we used a cyclic voltammetry technique and a mercury electrode (HMDE). In concordance with polarographic studies, at pH < 6 no signals were observed. However, from pH > 7.0 well-resolved cyclic voltammograms were obtained (Fig. 2A) with a shifting in the peak potential at increased pH. Studies at different sweep rates (0.1–10 V/s) indicated that NPD exhibited $\Delta E_p$ values of 42.5 ± 5.2 mV and 39.6 ± 2.9 mV for pH 9.0 and pH 12, respectively. From the above data, a quasi-reversible two-electron reduction process could describe the reduction of NPD because $\Delta E_p$ values does not fit completely to a reversible two-electron reduction process (30 mV). Therefore in this medium, the nitroso compound is reduced to the corresponding hydroxylamine derivative, according to:

$$\text{Ar-NO} + 2e^- + 2\text{H}^+ \rightleftarrows \text{Ar–NHOH} + \text{H}_2\text{O} \qquad (1)$$

Also, in Fig. 2B, the effect of sweep rate on the current ratio, $I_{pa}/I_{pc}$ at pH 9.0 and pH 12 is shown. As can be seen, at pH 9, current ratio is practically independent of sweep rate, indicating that under these conditions, no chemical reaction is present. In contrast, at pH 12, current ratio $I_{pa}/I_{pc}$ tends to a value of unity with increasing sweep rate. Therefore under this condition, the reduction is best described by an $EC_i$

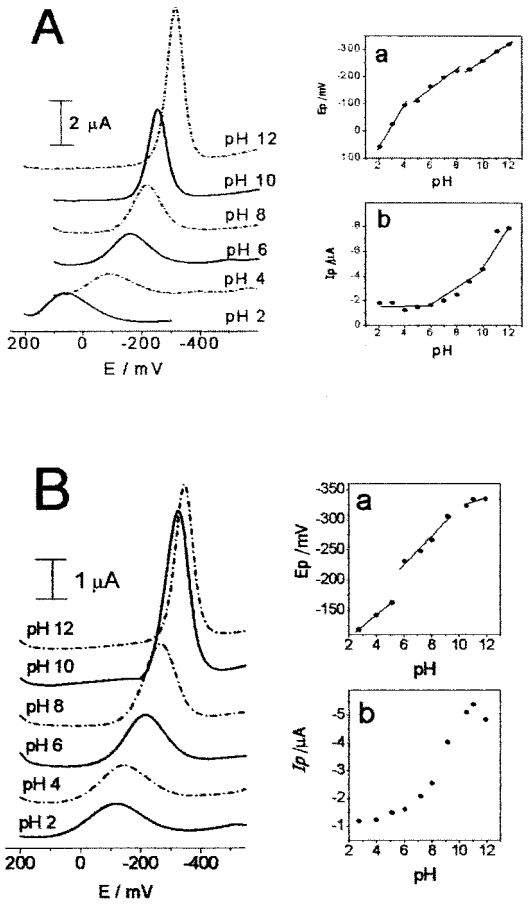


**Fig. 1.** Differential pulse voltammograms at different pH values of 0.1 mM NPD in (A) protic medium, 0.1 M Britton–Robinson buffer/ethanol: 70/30 + 0.3 M KCl and (B) mixed medium, 0.015 M aqueous citrate /DMF: 60/40, 0.3 M KCl and 0.1 M TBA perchlorate. Peak potential (plots a) and peak current (plots b) dependence of NPD behavior with pH in the corresponding media.

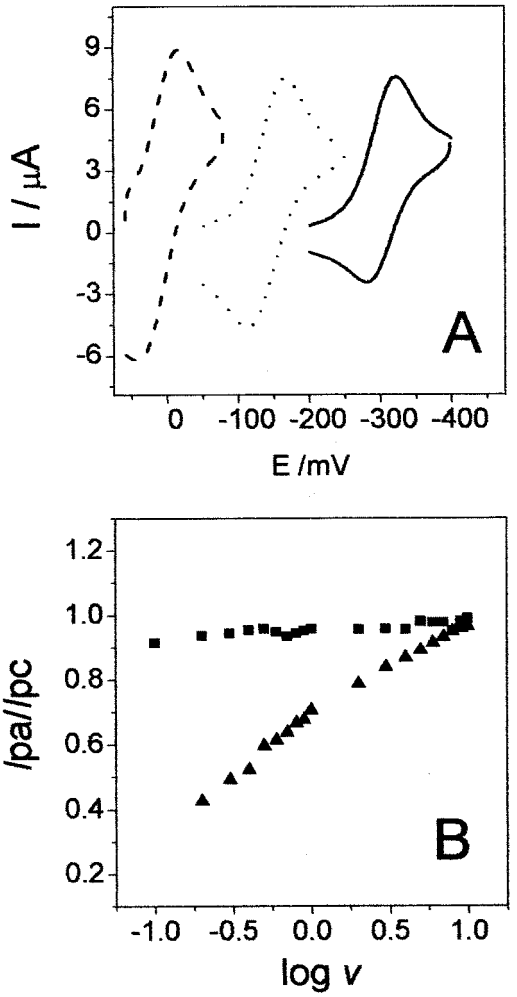


**Fig. 2.** (A) Cyclic voltammograms of 1 mM NPD in protic medium, 0.1 M Britton-Robinson buffer/ethanol: 70/30 + 0.3 M KCl at pH 6 (dashed line), 9 (dotted line), and 12 (solid line). Sweep rate 1 V/s. (B) Current ratio dependence on sweep rate for pH 9 (■) and pH 12 (▲).

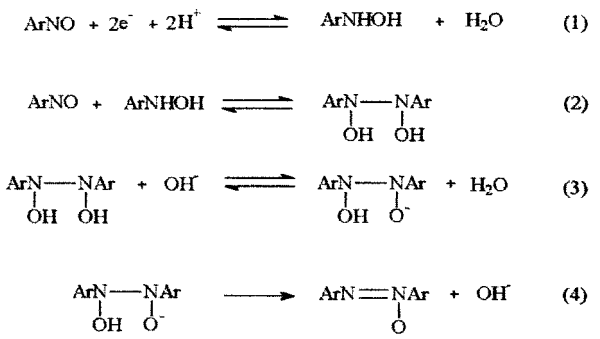


**Scheme I.** Electrodic mechanism of nitroso reduction of NPD in protic medium.

mechanism (10). These results are consistent with previous studies (18,19), which have reported the existence of a chemical reaction between the parent nitroso compound with the electrochemically formed hydroxylamine derivative. However, this reaction is highly favored only at strong alkaline pH. In consequence, the electrodic process for NPD in aqueous media corresponds to a mechanism described in Scheme I.

### Mixed Media

At pH < 6, NPD did not show any signal at DME in 0.015 M aqueous citrate/DMF: 60/40, 0.3 M KCl, and 0.1 M TBA perchlorate (TBAC). However, at pH > 6 NPD was reduced with a single well-defined signal in the DPP and Tast mode. The signal was shifted to more cathodic potentials with increasing pH within the range between pH 7–10 (77.7 mV/pH). From pH > 10, peak potential was pH independent. In tast polarography mode, the compound presented a similar dependence between $E_{1/2}$ and pH. Cathodic peak currents were pH-independent, and the peak areas remained unchanged with pH.

Studies on the reduction of NPD by differential pulse voltammetry on a glassy carbon electrode enabled us to electrochemically characterize NPD in the whole pH range as can be seen in Figure 1B. Results from this study did not show many differences with the above summarized results on the Hg electrode, i.e., a well-resolved peak in whole pH range, with the Ep-pH plot showing three linear segments with the following slopes: zone 1 (pH ≥ 2 to pH ≤ 5): 18.6 mV/pH, zone 2 (pH ≥ 6 to pH ≤ 9): 23.8 mV/pH and zone 3 (pH ≥ 9 to pH ≤ 12): 7.3 mV/pH.

To determine the electrode mechanism of NPD reduction in this medium at pH > 9, a Tast polarogram comparison of solutions at the same concentrations and pH of NPD derivative and nitrosobenzene were made. The obtained ratio of their limiting currents was close to 1, confirming that the reduction of this NPD derivative is due to a one-electron mechanism like nitrosobenzene (20)

Cyclic voltammetry was performed in the same electrolytic media as polarographic experiments. From pH 9, a well-resolved reversible couple for NPD derivative appeared at $E_{pc} = -353$ mV and $E_{pa} = -235$ mV (Fig. 3A). At pH 12, the following peak potential values were found: $E_{pc} = -354$ mV and $E_{pa} = -264$ mV (Fig. 3B). $\Delta E_p$ values for the couple at pH 9 were 118 ± 20 mV and of 90 ± 19 mV for pH 12, respectively. This result points out that the process corresponds to reduction of the nitroso derivative to give the ni-

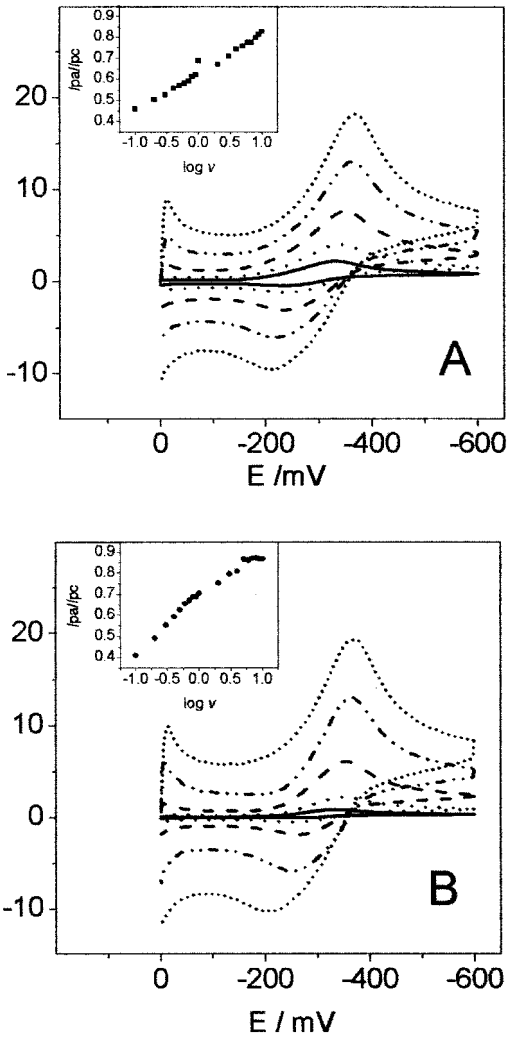


**Fig. 3.** Cyclic voltammograms of 1 mM NPD in mixed medium, 0.015 M aqueous citrate/DMF: 60/ 40, 0.3 M KCl, and 0.1 M TBA perchlorate at different sweep rates. (A) pH 9 and (B) pH 12. Insets: Current ratio dependence on sweep rate for each pH.

troso radical anion, involving the quasi-reversible one-electron transfer according to Eq. (2):

$$\text{Ar-NO} + e^- \rightleftarrows \text{Ar–NO}^- \qquad (2)$$

On the other hand, the $I_{pa}/I_{pc}$ ratio value increased concomitantly with increasing sweep rate (insert Fig. 3, A and B), indicating that the overall mechanism involves a chemical step after the electron transfer. Moreover, as predicted by Olmstead (12) for a second-order reaction, the $I_{pa}/I_{pc}$ ratio decreased parallel with increasing concentration of NPD at both pH 9 and 12. The cathodic peak potential also depends on NPD concentration (0.01–5 mM), with $dE_{pc}/d\log c$ values varying around 21 ± 3 mV. This value is in agreement with the theoretical value of 19.5 mV for an $EC_i$ process where the chemical step follows second-order kinetics (10).Then, according to work previously described by Kastening (21) and Asirvatham (22), this second-order chemical step corresponds to a dimerization process, according to the mechanism described in Scheme II.

The second-order rate constant was assessed from single

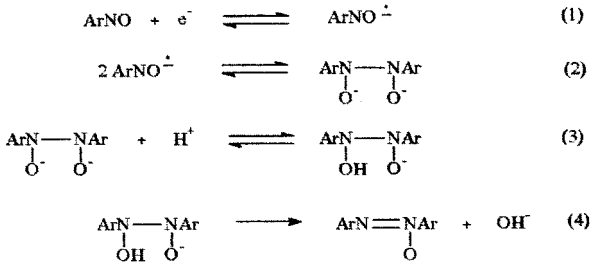


**Scheme II.** Electrodic mechanism of nitroso reduction of NPD in mixed and aprotic media.

voltammograms, according to Olmstead (12) from the following relationship:

$$\log \omega = \log (k_2 C_0 \tau) \quad (3)$$

From a plot of the kinetic parameter, ω, vs. the time constant, τ, the second order rate constant for the NPD derivative at pH 9 had an average, $k_2$ value of 11,300 ± 198 $(Ms)^{-1}$ .

### Aprotic Media

In this medium (dimethylformamide + 0.1 M TBAC) both in DPP mode and tast polarography, NPD exhibited only one main signal, with a peak potential value of –750 mV. By cyclic voltammetry, NPD exhibited a reversible couple with the following peak potential values: $E_{pc} = -768$ mV and $E_{pa} = -692$ mV at a sweep rate of 1V/s (Fig. 4). $\Delta E_p$ value for the couple was 76 ± 10 mV, indicating that a one-electron process is involved.

From the dependence between $I_{pa}/I_{pc}$ ratio with the logarithm of the sweep rate (Fig. 4B), it is clear that together with the one-electron transfer to give the nitroso radical anion, an irreversible chemical reaction followed, i.e., an ECi type of mechanism (12).

As was found in mixed media, the $I_{pa}/I_{pc}$ ratio decreased parallel with increasing NPD concentration. A plot of the kinetic parameter, ω, vs. the time constant, τ, was linear. The compliance of these criteria supports that the NPD reduction mechanism in this medium followed second order kinetics. Assuming a dimerization process, the calculated second order rate constant for the NPD derivative had an average $k_2$ value of 8,820 ± 198 $(Ms)^{-1}$.

To complete the characterization of the nitroso radical anion, UV-visible curves for the time–course of electrolysis of the NPD derivative were recorded at different time intervals. The original absorption at $\lambda_{max} = 314$ nm and $\lambda_{max} = 700$ nm decreased during CPE, but the band intensity at 262 nm increased. On the other hand, two isobestic points at 303 nm and 336 nm were also observed. The most relevant change in the original spectrum of NPD was the disappearance of the visible band $\lambda_{max}$ at 700 nm, which indicates reduction of the nitroso group. Furthermore, as a consequence of the electrolysis a significant change occurred in the color of the solution, turning from green to dark yellow. To evidence the appearance of new signals in the UV-Vis spectrum, the initial concentration of NPD derivative was increased 10 times compared with those required observing changes in the original bands. Thus, as can be seen from Fig. 5A, concomitantly with the time–course of electrolysis, a new visible band with a maximum at 390 nm was observed. This fact indicates that

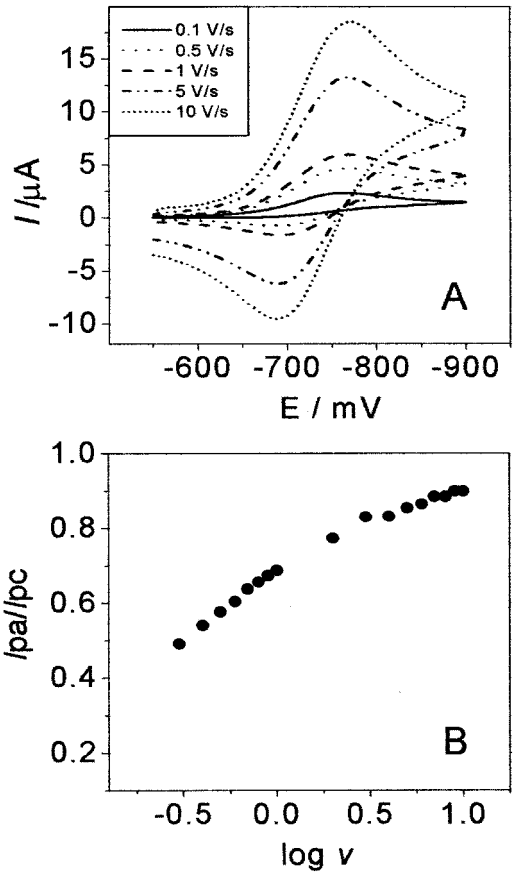


**Fig. 4.** (A) Cyclic voltammograms of 1 mM NPD in aprotic medium, 0.1 M TBA perclorate in DMF at different sweep rates. (B) Current ratio dependence on sweep rate for the same experiment.

there is a new species in solution, i.e., the nitroso radical anion. These experiments also were conducted in mixed medium with similar spectroscopic changes (data not shown).

### Digital Simulation

All the reduction mechanisms for nitroso groups were simulated using a DigiSim® CV simulator. For protic medium, two electrons, two-proton transfer mechanism was considered. Moreover, for pH 12, a chemical reaction according to scheme I was considered. For mixed and aprotic media, a one-electron transfer and chemical decay reactions were considered, according to Scheme II.

Some considerations were done to obtain each simulation: 1) all protonation reactions were assumed to be fast compared with the electrodic reactions and therefore to be at equilibrium; 2) the chemical decay mechanism in all media were considered as a single global reaction because for both mechanisms there exists only one irreversible reaction, [Eq. (4)], Schemes I and II); then, we used the experimental decay constant values obtained for each condition by cyclic voltammetry using the Olmstead theory; 3) finally, the value for the chemical reaction mechanisms in protic medium at pH 12 was obtained using the DigiSim software. Comparison between experimental with simulated cyclic voltammograms were consistent.

From the results we can corroborate: 1) in protic media the electron transfer has a quasi-reversible mechanism at both

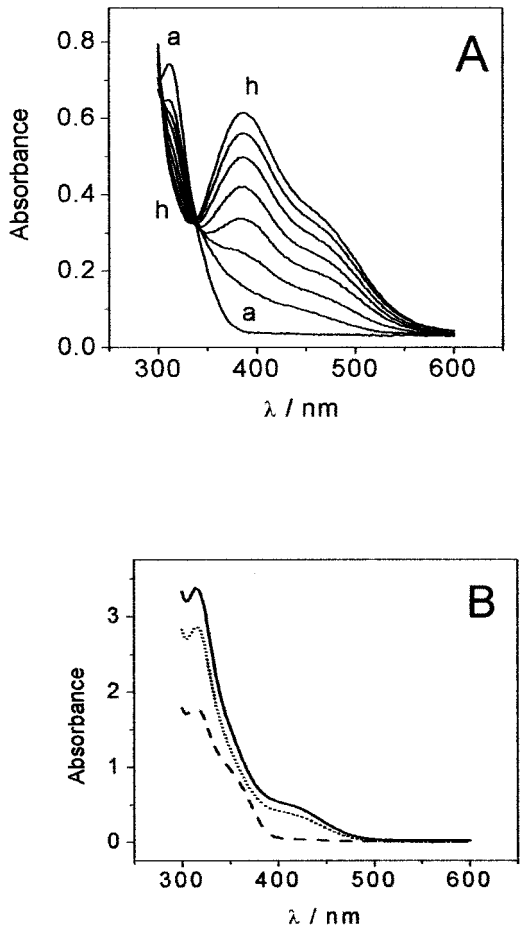


**Fig. 5.** (A) UV-Vis changes of 1 mM NPD in aprotic medium during electrolysis (a) before and (b–h) after each 5 min of electrolysis. Electrolysis potential: –1000 mV in aprotic medium. (B) UV-Vis spectra of 10 min electrolyzed 1 mM NPD solution in mixed medium without endo/xenobiotic (solid line) and in presence of 0.38 mM of *N*-acetylcysteine (dashed line) and adenine (dotted line). Electrolysis potential: –500 mV.

pH 9 and 12, but this quasi-reversibility is mainly dominate by the second electron transfer as is possible to observe from the heterogeneous constant range value ($k^0$) obtained. Also this condition is reflected in the $E^0$ values that do not coincide with the $E$p values; 2) in mixed and aprotic media, the $k^0$ and the $E^0$ values are coincident with quasi and reversible mechanisms, respectively; and 3) also in these media the experimental $k_2$ values permit us to simulate the voltammograms in good form, giving validity to the developed method. Moreover, we calculated an overall irreversible constant value for the reaction that occurs at pH 12 in protic media in $1.7 \times 10^4$ $(Ms)^{-1}$.

### Reactivity of the Nitro Radical Anion from NPD toward Endo/Xenobiotics of Pharmacologic Relevance

The optimal medium should provide a good stabilization and separation of the nitroso radical anion from other redox intermediates thus permitting us to study its reactivity with relevant biologic targets in isolation. The mixed media that fulfills the above characteristics was 0.015 M aqueous citrate, 0.3 M KCl / DMF (40/60), 0.1 M TBAC at pH 9.0. To test the reactivity of the nitroso radical anion from NPD with the proposed endobiotics (glutathione, adenine) and the xenobiotics (*N*-acetylcysteine, cysteamine) a six-step method was applied. First, cyclic voltammograms of each endo/xenobiotic were carried out in both the same voltage and sweep rates in which the nitroso radical appears. This study showed no peaks with any of the compounds assayed. Second, a comparison of different parameters of the cyclic voltammograms (i.e., $I_{pc}$, $I_{pa}$, $E_{pc}$, $E_{pa}$) was established. Third, the characteristic linear dependence between $\omega$ vs. $\tau$ for a second-order chemical reaction of the radical was obtained both in the absence ($k_2$) or in the presence of the endo/xenobiotics studied ($ki_{app}$). However, concomitant with the increase in the concentration of endo/xenobiotics, an increase in the slope of the plot was also observed, always keeping correlation coefficients greater than 0.98. This last effect could be explained by the contribution of two different simultaneous competitive decay pathways, i.e., the natural decay of the radical and its reaction with the endo/xenobiotics, which can be summarized as follows:

$$2\ \text{Ar-NO}^- + 2\text{H}^+ \xrightarrow{k_2} \text{Ar-N(O)} = \text{N-Ar} + \text{H}_2\text{O}$$

$$\text{Ar-NO}^- + \text{Endo/Xenobiotics} \xrightarrow{k_1} \text{Products}$$

Fourth, the effect of increasing concentrations of the studied compounds on the $I_{pa}/I_{pc}$ ratios of the radical at different sweep rates was assessed. Fifth, from the slopes of the plots of $\omega$ vs. $\tau$ in the presence of the endo/xenobiotics, the $ki_{app}$ values were calculated. Finally, from plots of $ki_{app}/2k_2$ vs. endo/xenobiotic concentrations and applying a previously described procedure (13,23), the interaction rate constants ($ki_{app}$) were obtained.

The effects of additions of endo/xenobiotics on the $I_{pa}/I_{pc}$ ratios demonstrated that parallel with an increase in the concentrations of such derivatives, a decrease in the current ratio at different sweep rates was observed (Fig. 6). From these results, cysteamine is the most potent derivative with a decrease in the Ipa/Ipc of 18.4%. The weakest effect corresponds to adenine (0.8%), at an NPD:endo/xenobiotic ratio of 5:1. On the other hand, at a similar concentration ratio (5:1), glutathione produced a decrease in the $I_{pa}/I_{pc}$ ratio of 6.2% and *N*-acetylcysteine of 3.3%. The interaction rate constants (calculated according to the procedure described in References 13 and 23) and their relationships to the reaction between the nitroso radical anion from NPD and the endo/xenobiotics at pH 9 are shown in Table I. From this table, it can be concluded that cysteamine shows the highest interaction rate constant ($ki_{app}$) as compared with all the other tested derivatives. Based on these results at pH 9, the following tentative order of reactivity can be established: cysteamine > *N*-acetylcysteine ≈ glutathione > adenine.

The reactivity of the nitroso radical anion from NPD with endo/xenobiotics, generating the radical by exhaustive electrolysis both in aprotic and in mixed media was also followed by UV-Vis spectroscopy. In general terms, the results from these experiments no significant differences in reactivity from those obtained in cyclic voltammetric experiments were found. In Figure 5B, the effects of addition of *N*-acetylcysteine and adenine after 10 min to electrolyzed NPD solutions in mixed medium is illustrated. As can be seen, the UV-Vis band at 425 nm corresponding to the nitroso radical

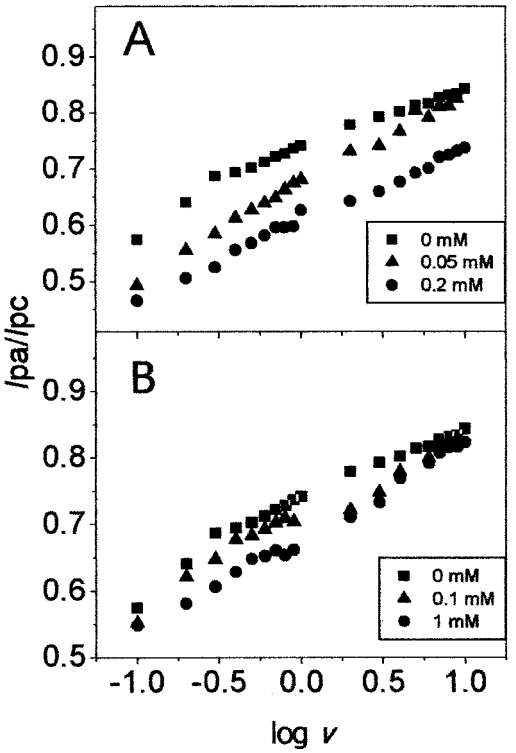


**Fig. 6.** Effect of adding (A) cysteamine and (B) glutathione on the current ratio dependence and the sweep rate for 1 mM NPD in mixed medium.

anion disappeared after the addition of *N*-acetylcysteine. A similar effect was observed with cysteamine and glutathione, with no significant differences between them. In contrast, adenine produced little decrease of the intensity of the band, consistent with the reactivity found in CV experiments.

In Table II, a comparison of reactivity between free radicals from NPD with the parent drugs, nifedipine and flutamide are presented. As can be seen, as expected under these experimental conditions NPD was reduced at less cathodic potentials than the nitro compounds. In general terms, nitro radicals were significantly more stable than nitroso radical from NPD, i.e., 46.6 and 4.4 times for nifedipine and flutamide, respectively. On the other hand, nitroso radical was the most reactive species towards xeno/endobiotics. Our results document that free radicals from NPD could be the most cytotoxic species, considering both its ease of formation and the reactivity towards the tested biologic targets.

**Table I.** Interaction Rate Constants ($k_i$) for the Reactivity between Nitro Radical Anion from Flutamide Electrochemically Generated and Endo/Xenobiotics of Pharmacological Relevance at pH 9.0 and a Sweep Rate of 1 V/s

| Endo/xenobiotic | $k_i\ (Ms)^{-1} \times 10^4$ | $k_i k_2$[a] | $k_{icys}/k_{endo/xeno}$[b] |
|---|---|---|---|
| Glutathione | 4.3 | 3.8 | 38.1 |
| Cysteamine | 164 | 145.1 | 1 |
| N-acetylcysteine | 4.72 | 4.2 | 34.7 |
| Adenine | 1.62 | 1.5 | 101.2 |

[a] Second order decay constant ($k_2$) = 11,300 at pH 9.0.

[b] Constant ratio between the interaction rate constant for cysteamine and the interaction rate constants for the other tested endo/xenobiotics

**Table II.** Electrochemical Characteristics of the Radical Anions Electrochemically Generated from Nitro- and Nitroso-Compounds and Their Reactivities with Pharmacologically Relevant Targets in Mixed Media at pH 9.0

| Derivative | –Ep, mV | $k_2\ (Ms)^{-1}$ | GSH | Cysteamine $k_i\ (Ms)^{-1} \times 10^{-4}$ | Adenine |
|---|---|---|---|---|---|
| NPD | 353 | 11,300 | 4.3 | 1,640 | 1.62 |
| Nifedipine | 1,089 | 265 | 1.71 | 2.68 | 1.25 |
| Flutamide | 820 | 2,560 | 0.96 | 1.55 | 0.53 |

## ACKNOWLEDGMENTS

The authors gratefully acknowledge the financial support of FONDECYT Lineas Complemetarias (grant 8000016).

## REFERENCES

1. P. D. Henry. Comparative pharmacology of calcium antagonists: nifedipine, verapamil and diltiazem. *Am. J. Cardiol.* **46**:1047–1058 (1980).
2. P. Jakobsen, O. Lederballe Pedersen, and E. Mikkelsen. Gas chromatographic determination of nifedipine and one of its metabolites using electron capture detection. *J. Chromatogr.* **162**:81–87 (1979).
3. B. K. Logan and K. S. Patrick. Photodegradation of nifedipine relative to nitrendipine evaluated by liquid and gas chromatography. *J. Chromatogr.* **529**:175–181 (1990).
4. Y. Matsuda, R. Teraoka, and I. Sugimoto. Comparative evaluation of photostability of solid-state nifedipine under ordinary and intensive light irradiation conditions. *Int. J. Pharmaceutics* **54**: 211–221 (1989).
5. M. Morad, Y. E. Goldman, and D. R. Trentham. Rapid photochemical inactivation of Ca2+-antagonists shows that Ca2+ entry directly activates contraction in frog heart. *Nature* **304**:635–638 (1983).
6. R. Teraaka. Y. Matsuda and Sugimoto. Quantitative design for photostabilization of nifedipine by using titanium dioxide and/or tartrazine as colorants in model film coating systems. *J. Pharm. Pharmacol* **41**:293–297 (1988).
7. N. K. Gibbs. N. J. Traynor, B. E. Johnson, and J. Ferguson. *In vitro* photostability of nifedipine: sequential induction of toxic and non-toxic photoproducts with UV-A radiation. *J. Photochem. Photobiol. B.* **13**:275–288 (1992).
8. N. Hayase. Y-I. Itagaki., S. Ogawa., S. Akutsu, and S-I. Y. Abiko. Newly discovered photodegradation products of nifedipine in hospital prescriptions. *J. Pharm. Sci.* **83**:532–538 (1994).
9. R .S. Nicholson. Semiempirical procedure for measuring with stationary electrode polarography rates of chemical reactions involving the product of electron transfer. *Anal. Chem* **38**:1406 (1966).
10. G. Bontempelli, F. Magno, G. Mozzochin, and R. Seeger. Linear sweep and cyclic voltammetry. *Annali di Chimica.* **79**:138–147 (1989).
11. M. L. Olmstead and R. G. Hamilton. and R.S. Nicholson Voltammetry Theory for the Disproportionation Reaction and Spherical Diffusion. *Anal. Chem* **41**:260–266 (1969).
12. M. L. Olmstead, R. G. Hamilton, and R. S. Nicholson. Theory of cyclic voltammetry for a dimerization reaction initiated electrochemically. *Anal. Chem.* **41**:260–266 (1969).
13. L. J. Núñez-Vergara, F. García, M. M. Domínguez, J. De la Fuente, and J. A. Squella. In situ reactivity of the electrochemically generated nitro radical anion from nitrendipine with glutathione, adenine and uracil. *J. Electroanal. Chem.* **381**:215–219 (1995).
14. L. J. Núñez-Vergara. J. C. Sturm, A. Alvarez-Lueje, C. Olea-Azar, C. Sunkel, and J.A. Squella electrochemical oxidation of 4-methyl-1,4-dijydropyridines in protic and aprotic media. *J. Electrochem. Soc.* **146**:1478–1485 (1999).

15. A. G. Gonzalez, F. Pablos, and A. Asuero. Corrections Factors for the glass electrode revisited. *Talanta* **39**:91 (1992).
16. A. G. Asuero and M. A. Herrador, and A.G. González,, Estimation of pH and autoproteolysis constants in mixtures of aliphatic amides with water: medium effect on the 4-aminobenzene system. *Talanta* **40**:479–484 (1993).
17. E. Laviron, A. Vallat, and R. Meunier-Prest, The reduction mechanism of aromatic nitro compounds in aqueous medium Part V. The reduction of nitrosobenzene between pH 0.4 and 13. *J. Electroanal. Chem.* **379**:427–435 (1994).
18. J. H. Tocher. R. C. Knigth, and D. I. Edwards. Electrochemical characteristics of nitro-heterocyclic compounds of biologic interest. II. Nitrosochoramphenicol. *Free Rad. Res. Commun.* **5**:319–326 (1989).
19. A. Streitwiesser and C. H. Heatcock. In: Química Orgánica, Interamericana, (1996).
20. P. Zuman and S. Bhavdeep. Addition, reduction, and oxidation reactions of nitrosobenzene. *Chem Rev.* **94**:1621–1641 (1994).
21. B. Kastering. P. L. Meites, I. M. Kolthoff. In Zuman (ed.), Progress in Polarography, vol 3, John Wiley & Sons, New York, 1972 pp. 259–266.
22. M. R. Asirvatham and D. Hawley. Electron-transfer processes: the electrochemical and chemical behavior of nitrosobenzene. *J. Electroanal. Chem.* **57**:179–190 (1974).
23. L. J. Núñez-Vergara, M. E. Ortiz, S. Bollo, and J. A. Squella. Electrochemical generation and reactivity of free radical redox intermediates from ortho-and meta-nitro substituted 1,4-dihydropyridines. *Chem. Biol. Interact.* **106**:1–14 (1997).